地 震 研 究 所 彙 報
Bull. Earthq. Res. Inst.
Univ. Tokyo
Vol. 81 (2006) pp. 309–315

Site Effects Derived from Spectral Inversion Method for K-NET, KiK-net, and JMA Strong-Motion Network with Special Reference to Soil Nonlinearity in High PGA Records

Hiroshi Kawase*

Faculty of Human-Environment Studies, Kyushu University

Abstract

In this study we first try to separate so-called source spectra, attenuation coefficient, and site amplification factors from K-Net, KiK-net, and JMA strong-motion (Shindo-kei) network records observed throughout Japan. As a reference site, we use one rock station of KiK-net, and we remove a very small site effect caused by weathered layers from the record using 1-D theoretical amplification. Once we obtain site amplification factors, we try to obtain nonlinear site factors for high PGA records observed during the 2003 Tokachi-Oki earthquake as a ratio of the observed record with respect to the hypothesized input bedrock motion calculated as an average from small PGA (i.e., less than 200 Gals) records. When we compare these site effects with linear site effects for smaller PGA records, we find that several sites show lower peak amplitude with lower peak frequency than expected from previous studies. However, at a few very soft sites we found higher peak amplitude with lower peak frequency. This phenomenon can be interpreted to occur as the impedance effect (makes amplitude higher) is strengthened by nonlinearity, and overcomes the damping effect (makes amplitude lower).

Key words : Spectral inversion, nonlinearity, site effects, strong motion, PGA

1. Introduction

In this study we first try to separate so-called source spectra, attenuation coefficient, and site amplification factors from K-Net, KiK-Net, and JMA Shindokei network records observed throughout Japan. The Fourier Spectra separation method (i.e., spectral inversion method) is the well-established one of Andrews (1981) with a fixed reference site. For the reference site, we use one rock station of KiK-Net in Yamaguchi Prefecture, that is, YMGH01, from which we remove the effects of shallow surface deposits. Once we obtain site amplification factors, we try to obtain nonlinear site factors for high PGA (i.e., larger than 200 Gals) records observed during the 2003 Tokachi-Oki earthquake as a ratio of the observed record with respect to the hypothesized input bedrock motion calculated as an average from small PGA (i.e., less than 200 Gals) records. This process can derive nonlinear soil amplification factors in comparison to linear factors as long as the source and path effects are successfully modeled by separated characteristics.

2. Reference Site

A simple spectral inversion method needs one additional constraint for separating source, path, and site factors. There are many variations, but physically the simplest constraint is to take one station as a reference site. This means that this reference site has no amplification as an effect of surface geology, and the resultant source and site factors will be relative to this reference site. If there is a site effect at this site, then the deviation from true reference will be mapped onto all of the source and site factors

* e-mail: Kawase@arch.kyushu-u.ac.jp (6–10–1 Hakozaki, Higashi-ku, Fukuoka, 812–8581, Japan)

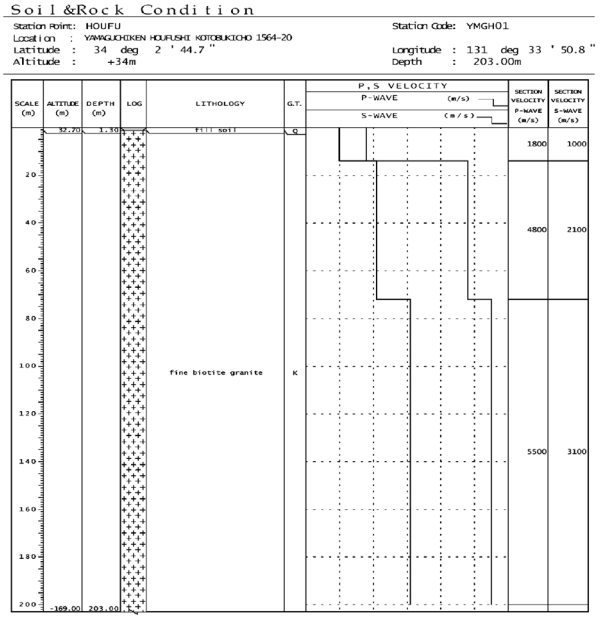

Fig. 1. Soil profile at YMGH01 KiK-net site (http:// http://www.kik.bosai.go.jp/kik/)

in the opposite (i.e., canceling-each-other) manner. Thus, the success of separation solely depends on a good choice of reference site. Thanks to the wide range of sites selected for KiK-net and its borehole station deployment, we can find several good candidates for the reference site among about 500 KiK-net sites. After the preliminary analysis of the spectral inversion, we search for the best reference site based on the separated site amplification factors, S-wave velocity of the borehole logging (open to the public at http://www.kik.bosai.go.jp/kik/index_en.shtml), and numbers of observed data. We choose YMGH01 because it has very high S-wave velocity layers below, as shown in Fig. 1, and quite a small site effect. We also have sufficient numbers of strong motion records here. At the site we have a borehole sensor 200 m below the surface.

Although this is a site with a rock outcrop, we have two weathered layers as seen in Fig. 1. Because amplification due to these weathered layers near the surface is small, but not negligible, it would be better to remove the amplification for these layers. Before removing amplification based on 1-D wave propagation theory we invert the S-wave velocity structure for the optimal result through the so-called Genetic Algorithm using amplitude and phase of the transfer function between borehole (−200 m) and surface sensors. Fig. 2 shows matching amplitude and phase of

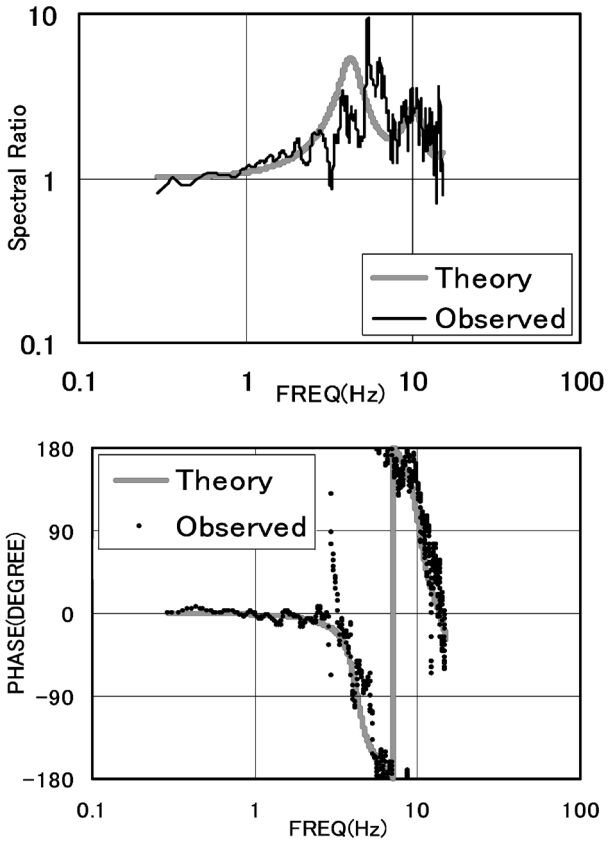

Fig. 2. Comparison of amplitude and phase (observed and inverted) at YMGH01

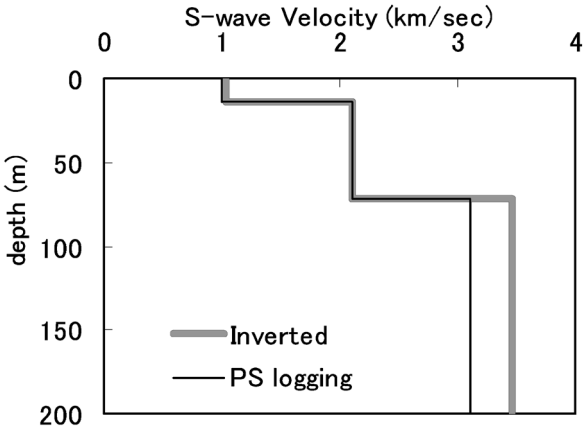

Fig. 3. Original and inverted S-wave velocity profiles at the reference site YMGH01

the averaged transfer functions of observed data with 1-D theory with vertical incidence of S-wave. We found that the S-wave velocity of the basement rock reaches 3.4 km/sec as shown in Fig. 3. The observed spectra at this reference site are corrected using theoretical amplification from the outcrop of the 3.45 km/sec layer to the surface.

3. Data and Method of Analysis

We jointly use K-NET, KiK-net, and JMA Shindokei network as a source of weak motions in Japan. K-NET started operation from May 1996 with 1000 surface stations, while KiK-net started operation from June 1997 with about 500 surface and downhole stations (at present 660 stations). K-NET stations have P-S logging velocity profiles up to 20 m (http://www.k-net.bosai.go.jp/k-net/), while KiK-net stations have those up to the depths of downhole stations, usually 100 m to 200 m, except for 21 sites inside sedimentary basins for which we have more than 1000 m (See again KiK-net web site). We also use weak motion data from the JMA Shindokei network, which was designed to quickly broadcast JMA seismic intensity, and started operation from October 1996. JMA stations do not have any information on their site conditions, yet.

We collect not so strong and weak motion records observed by these three strong motion networks from August 1996 to June 2002. After the Tokachi-Oki earthquake of September, 27, 2003, we add main shock and major aftershock records to the database. Criteria to select appropriate earthquakes and data are: i) Mjma$\geqq$4.5, ii) depth$\leqq$60 km, iii) hypocentral distances X$\leqq$200 km, iv) PGA$\leqq$200 Gals, v) triggered station$\geqq$3 par earthquake, and vi) earthquakes $\geqq$3 par site. By selecting observed records in this way final sites for inversion that can be connected by at least one common earthquake are 1700 in total, 913 from K-NET, 468 from KiK-net, and 319 from JMA network, and final earthquakes used are 261 (of which 33 are main shock and aftershocks of the Tokachi-Oki earthquake of 2003). The total number of source-station pairs is less than 20000. We can divide these 261 earthquakes into three categories, namely, plate boundary earthquake B (99+33), intraplate (slab) earthquake I (81), and inland crustal earthquakes C (48). We show locations and mechanisms of the target earthquakes from 1996 to 2002 in Figs. 4 to 6 and those of the 2003 Tokachi-Oki earthquake sequence in Fig. 7.

To analyze data, first we cut out the target accelerograms from the onset of S-wave with the duration of 5 seconds (M$<$6), 10 seconds (M$<$7), or 15 seconds (M$>$7). We use the standard travel timetable used by JMA, and it works quite well. Then, we calculate the Fourier spectra of these accelerograms. For Fourier spectra *Fij* for i-th earthquake observed at j-th site, we use the following equation:

$$\log F_{ij} = \log S_i - n_{l(i)} \log X_{ij} + \sum_k b_{l(i)k} X_{ijk} + \log G_j \quad (1)$$

$$X_{ij} = \sum_k X_{ijk} \quad (2)$$

where, Si is the source spectrum for i-th earthquake, Gj is the site factor for j-th site, Xij is the direct hypocentral distance for that pair, k is a region number with different attenuation, l(i) is source type (B, I, or C). We use both parameters for geometrical spreading n and intrinsic and scattering attenuation b. To delineate different attenuation characteristics at different regions in Japan, we divide Japan into six regions, as shown in Fig. 8, in which we assume a different attenuation coefficient b. We also assume that these parameters n and b are source-type dependent. The reason we introduce n as a separation parameter is to explain small attenuations in the intermediate distance range for shallow crustal earthquakes. We assume constant n equal to 1 for distance from 0 to 100 km.

4. Results

4. 1 Attenuation

As for the attenuation characteristics we found basically the same characteristics obtained without strong motion data by the 2003 Tokachi-Oki earthquake sequence (Kawase and Matsuo, 2002). As an example we show in Fig. 9 Q^{-1} values translated from the attenuation coefficients b for six regions, and in Fig. 10 the geometrical spreading factors n for different distance ranges for plate-boundary earthquakes.

4. 2 Source spectra

As for the source characteristics, we found inverted source spectra follow ω^{-2} curves so that we can translate them into a single parameter (=fc) ω^{-2} model. From corner frequency fc we can obtain Brune's stress drop. Fig. 11 shows stress drops of all the plate-boundary earthquakes. We found that stress drops for Hyuga-nada, Kyushu earthquakes (■) are slightly lower than those on average in Japan (●). We also found that the stress drops of the Tokachi-Oki earthquake sequence (▲) are on average similar to those of the other Pacific Plate (northern Honshu) earthquakes. The main shock is the exception whose stress drop reach 1000 bars, which seems too high. Because our analyzed frequency band is from 0.33 Hz

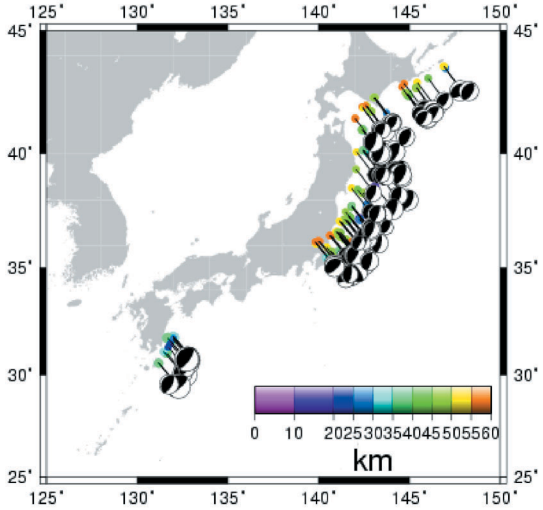

Fig. 4. Locations of plate boundary earthquakes

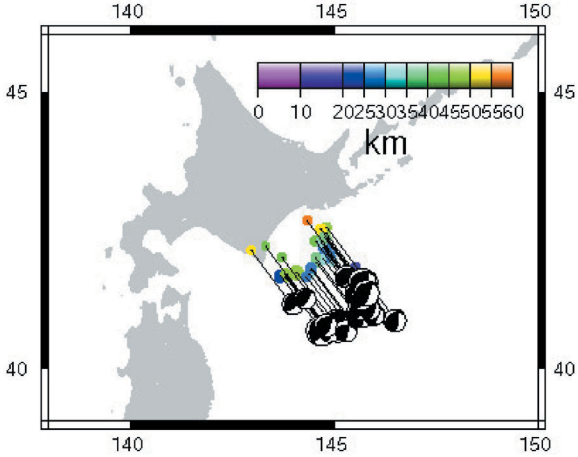

Fig. 7. Locations of main shock and aftershocks

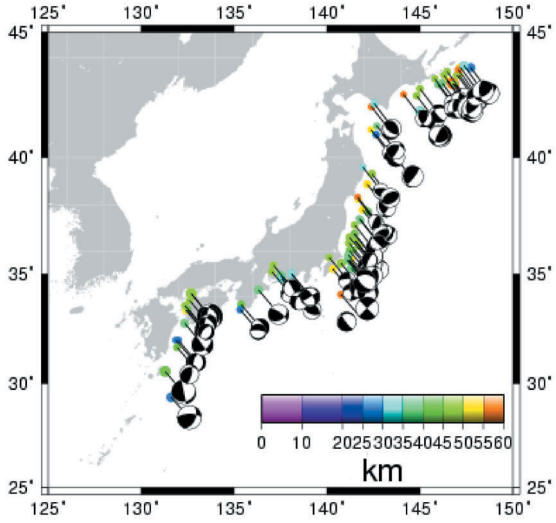

Fig. 5. Locations of intraplate earthquakes

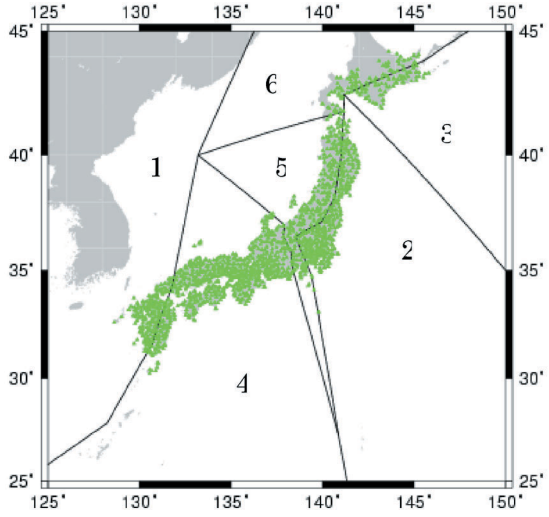

Fig. 8. Regions for different attenuation factors

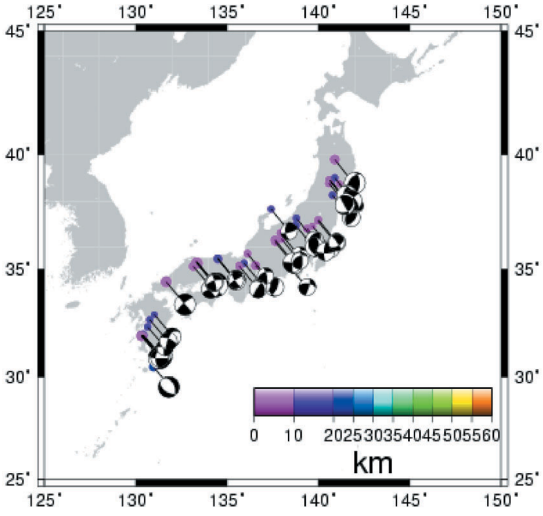

Fig. 6. Locations of crustal earthquakes

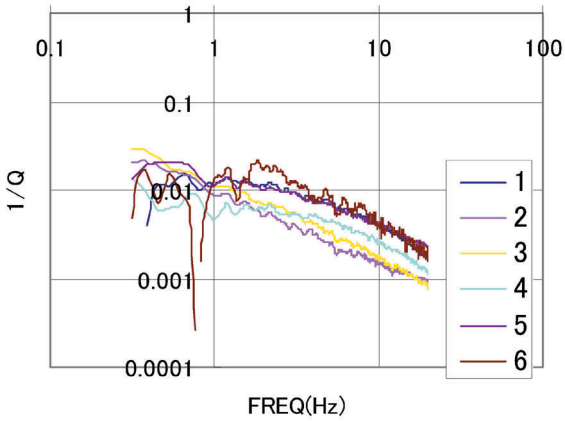

Fig. 9. Attenuation Q-1 for plate boundary earthquakes. Regions 1, 5, and 6 show high attenuation.

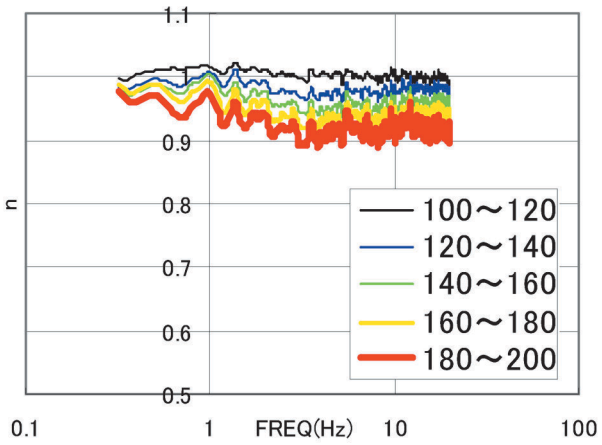

Fig. 10. Geometrical spreading factor n for plate boundary earthquakes. From 0 to 100 km we assume a fixed value, 1.0.

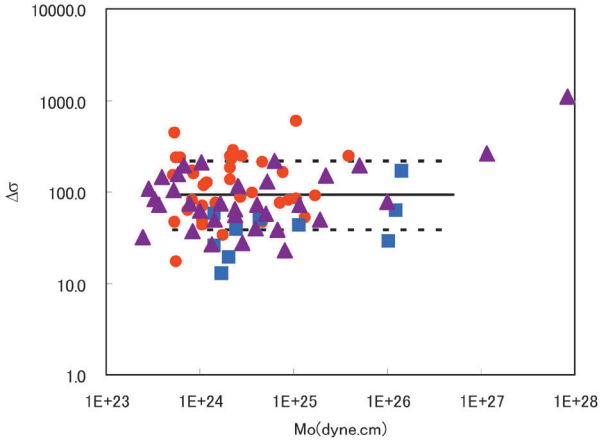

Fig. 11. Stress drops derived from inverted source spectra based on the Brune's model.

to 20 Hz and fc of the main shock should be less than 0.1 Hz, we should take this value as the upper boundary.

4. 3 Site factors

We have obtained site amplification factors at 1700 points throughout Japan with a variety of soil conditions. Once we have obtained weak motion site factors, we can obtain strong motion site factors by dividing observed spectra by modeled bedrock spectra. Thus, the nonlinearity that we can delineate from the comparison of these two site factors at the same site is the nonlinearity of all sediments from the bedrock, not the shallow surface soil layers where nonlinearity would be most prominent. Fig. 12 shows a comparison of site factors obtained from high (>200 Gals) and low PGA records. Red lines are

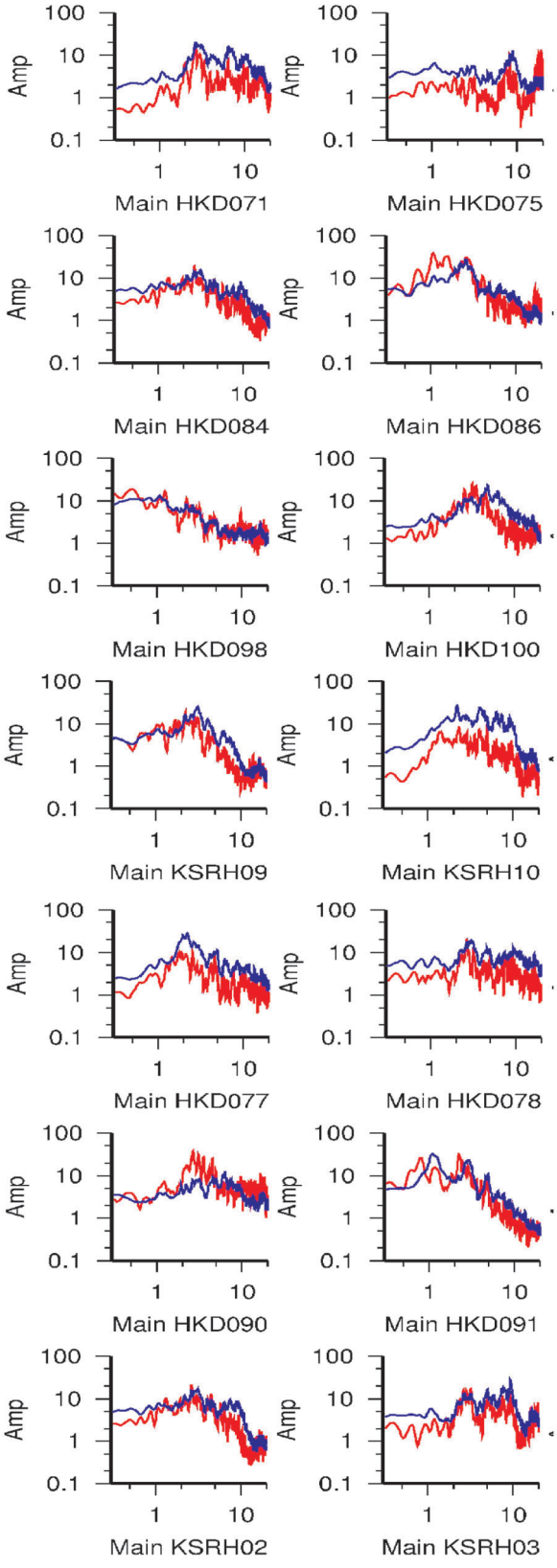

Fig. 12. Comparison of site factors derived from weak PGA (<200 Gals) records (smooth and blue) and from strong (>200 Gals) records (jaggy and red).

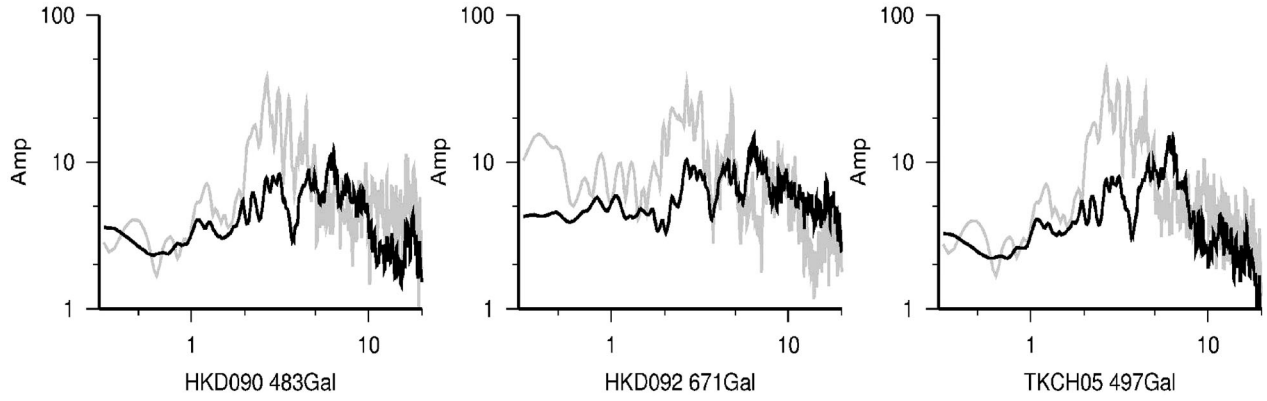

Fig. 13. Three very prominent sites of nonlinearity. Black lines are site factors for weak motions and gray lines are those for strong motions. Peak frequencies are lower, but peak amplitudes are higher for strong motions.

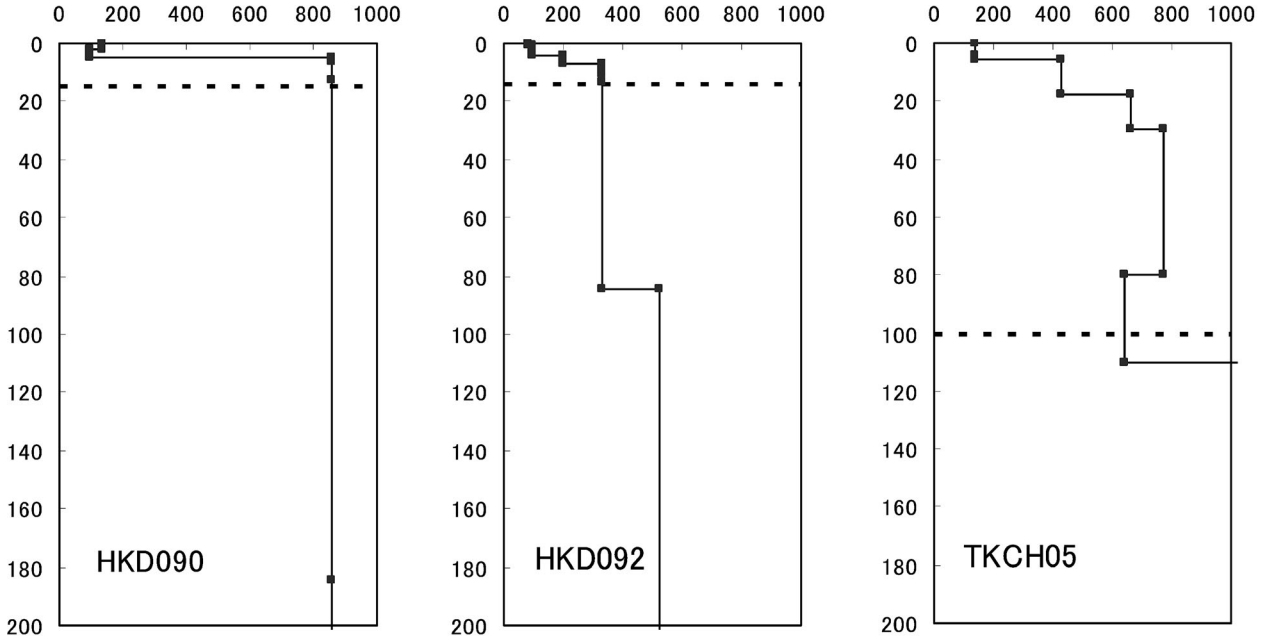

Fig. 14. S-wave velocity structures for three sites shown in Figure 13. Those above the dotted lines are obtained directly from borehole measurements, and those below are derived from the GA inversion by assuming 1-D wave propagation theory.

for high PGA records. We found that some of the sites do not show any significant difference, while the majority of sites show either lower peak frequency or lower peak amplitude. However, in our study we cannot find a site with typical characteristics of nonlinearity, namely, a lower peak amplitude at a lower peak frequency. Instead, we found several sites with a high peak amplitude at lower peak frequency. Fig. 13 shows three very prominent examples of such characteristics.

At these sites S-wave velocities of very shallow surface layers show quite low values, while layers just below have relatively high S-wave velocities. Fig. 14 shows S-wave velocity distributions for these three sites. Above the dotted lines S-wave velocities are directly measured by P-S logging inside the borehole, while below the dotted lines they are inverted using a Genetic Algorithm with the assumption of a vertical incidence of the S-wave. High peak amplitudes at these sites during strong shakes from the main shock would be caused by a strong velocity contrast at the topmost layers; nonlinearity lowers the S-wave velocity of the soft surface layer, so the impedance contrast between the surface layer and

the layer below becomes larger, and amplification becomes larger. The damping effect would be small because the thickness of the soft layer is quite small.

5. Conclusions

We obtained nonlinear site factors by calculating bedrock spectra only from relatively weak motions during the main shock of the Tokachi-Oki earthquake, and then took the ratios of strong motion spectra with respect to the spectra of the hypothesized bedrock motion at the sites. We found that some of the target sites show no significant nonlinearity, but that most of the sites show nonlinear site factors, namely, lower peak frequency and higher amplitude. When we checked the S-wave velocity structures at those sites with significant site factors, we found that they share similar S-wave velocity structures; S-wave velocity of topmost layer is quite low while bottom of that layer has quite a high S-wave velocity. If the effects of impedance contrast are stronger than the effects of damping due to strong shaking, then peak amplitude would be higher than in the linear calculation.

Acknowledgments

This study is partially supported by the Special Project for Earthquake Disaster Mitigation in Urban Areas from the Ministry of Education, Culture, Sports, Science and Technology of Japan. Special thanks are given to Mr. Hidenori Matsuo who helped the author to analyze the data. The author also appreciates the support of Prof. H. Takenaka of Kyushu University for his review comments and Prof. R. Kobayashi of Kagoshima University for his patience and encouragement to revise the manuscript.

References

Andrews, D.J., 1981, Separation of source and propagation spectra of seven Mammoth Lakes aftershocks, Proc. of Workshop XVI, Dynamic Characteristic of Faulting, USGS Open File Report.

Hiroshi Kawase and Hidenori Matsuo, 2004, Amplification Characteristics of K-NET, KiK-NET, and JMA Shindokei Network Sites Based on the Spectral Inversion Technique, 13th World Conference on Earthquake Engineering, Vancouver, Canada, Paper No. 454.

(Received December 23, 2005)
(Accepted January 15, 2007)